Modelling long-term (300ka) upland catchment response to multiple lava damming events

van Gorp, W.; Temme, A. J. A. M.; Veldkamp, A.; Schoorl, J. M.

IMPORTANT NOTE: You are advised to consult the publisher's version (publisher's PDF) if you wish to cite from it. Please check the document version below.

Document Version
Publisher's PDF, also known as Version of record

Publication date:
2015

[Link to publication in University of Groningen/UMCG research database](#)

Modelling long-term (300 ka) upland catchment response to multiple lava damming events

W. van Gorp,[1]* A. J. A. M. Temme,[1] A. Veldkamp[2] and J. M. Schoorl[1]
[1] Soil Geography and Landscape group, Wageningen University, P.O. box 47, 6700 AA Wageningen, The Netherlands
[2] Faculty ITC, University of Twente, P.O. Box 217, 7500 AE Enschede, The Netherlands

*Correspondence to: W. van Gorp, Soil Geography and Landscape group, Wageningen University, P.O. box 47, 6700 AA Wageningen, The Netherlands. E-mail: Wouter. vangorp@wur.nl

ESPL

Earth Surface Processes and Landforms

ABSTRACT: Landscapes respond in complex ways to external drivers such as base level change due to damming events. In this study, landscape evolution modelling was used to understand and analyse long-term catchment response to lava damming events. PalaeoDEM reconstruction of a small Turkish catchment (45 km^2) that endured multiple lava damming events in the past 300 ka, was used to derive long-term net erosion rates. These erosion rates were used for parameter calibration and led to a best fit parameter set. This optimal parameter set was used to compare net erosion landscape time series of four scenarios: (i) no uplift and no damming events; (ii) no uplift and three damming events; (iii) uplift and no damming events; and (iv) uplift and three damming events. Spatial evolution of net erosion and sediment storage of scenario (iii) and (iv) were compared. Simulation results demonstrate net erosion differences after 250 000 years between scenarios with and without dams. Initially, trunk gullies show less net erosion in the scenario with damming events compared with the scenario without damming events. This effect of dampened erosion migrates upstream to smaller gullies and local slopes. Finally, an intrinsic incision pulse in the dam scenario results in a higher net erosion of trunk gullies while decoupled local slopes are still responding to the pre-incision landscape conditions. Sediment storage differences also occur on a 100 ka scale. These differences behaved in a complex manner owing to different timings of the migration of erosion and sediment waves along the gullies for each scenario. Although the specific spatial and temporal sequence of erosion and deposition events is sensitive to local parameters, this model study shows the manner in which past short-lived events like lava dams have long-lasting effects on catchment evolution. Copyright © 2014 John Wiley & Sons, Ltd.

KEYWORDS: upland catchment; LAPSUS; lava dams; sediment storage; long-term response

Introduction

It has been recognized that geomorphic systems usually respond in complex nonlinear ways to external drivers such as climate or base level and that internal system dynamics exist even in the absence of external forcing (Schumm, 1979; Phillips, 2006). Landscape evolution models (LEMs) allow simulation of this complexity and nonlinearity. However, model results have to be analysed with caution owing to uncertainties in input data, spatial and temporal scale issues, simplifications in process descriptions and calibration and validation issues (Van De Wiel *et al.*, 2011). Furthermore, outputs of LEMs demonstrate this complexity and the necessity to acknowledge the significance of initial conditions, topography and historical contingency (Wainwright, 2006; Coulthard *et al.*, 2007). Although different modelling studies using reconstructed palaeo-landscapes (palaeoDEMs) have yielded successful results in reconstructing sediment volumes or landform patterns (Peeters *et al.*, 2008; Temme and Veldkamp, 2009; Baartman *et al.*, 2012b), large uncertainties remain. In particular, the lack of information about palaeo landscapes and the associated lack of data to validate model inputs and outcomes remain challenging for this approach.

Despite these limitations, frameworks emerge that landscape evolution modellers can use to simulate landscape response. Temme *et al.* (2011) argue among others that decisions on model setup and which processes to incorporate are case-specific and should be consciously made and tested. Tucker (2009) stresses that modelling landscape change of actual landscapes requires: (i) that only one variable, such as base level, changes significantly, while the rest remains fairly constant; (ii) needs temporal control on palaeosurfaces or rates of change; (iii) demands knowledge of the main processes active; and (iv) requires elevation data of sufficient quality. Van De Wiel *et al.* (2011) similarly emphasize the value of numerical models to test different external forcing scenarios of which results can be compared. All these workers stress that the introduction of too many parameters or too detailed process descriptions in landscape evolution studies is not desirable because it increases uncertainty of model outputs. Owing to these limitations the aim of such studies should not be an exact reconstruction of elevations or sediment thicknesses at specific locations. Better, general patterns of landscape change such as catchment sediment yields, river profile development, and general sediment redistribution patterns through time and space should be used to constrain model parameters and to

inform choices between model versions (Tucker and Hancock, 2010; Temme *et al.*, 2011). This line of reasoning can be extended by arguing that model simulations that aim to clarify the effect of external drivers, such as lava dams, on landscape evolution are more robust when based on actual landscapes with known geomorphic setting and validation data than on entirely fictitious landscapes.

Many landscape evolution modelling studies have investigated landscape response to external drivers (Tucker *et al.*, 2001; Coulthard *et al.*, 2005; Temme *et al.*, 2009; Hancock and Coulthard, 2012). The main advantage of using landscape evolution models (LEMs) for this purpose is the possibility to analyse landscape evolution on spatial and temporal scales beyond the limitations of fieldwork or laboratory based experiments. One of the specific cases where LEMs can be useful is the modelling of long-term landscape response to temporary damming, blocking and dam removal. These damming events are interesting from a geomorphological viewpoint because they have significant influence on river profile evolution, for instance in the case of landslide dams (Korup *et al.*, 2006, 2010) and could divert drainage of channels and entire river catchments, exemplified by different lava-dam studies (Roach *et al.*, 2008; Veldkamp *et al.*, 2012; Maddy *et al.*, 2012). Furthermore, LEMs are potentially valuable to increase knowledge on long-term response to human induced dammings and dam removals (Sawaske and Freyberg, 2012). Dams can either breach suddenly, leading to extreme flooding events (Fenton *et al.*, 2006), or can be incised gradually, temporarily hampering fluvial incision (Ely *et al.*, 2012). Response to damming is not necessarily straightforward. Besides the known effects of sediment deposition and knickpoint creation, damming can lead to complex responses such as stream rerouting and complex river profile evolution (Ely *et al.*, 2012; Maddy *et al.*, 2012; Van Gorp *et al.*, 2013).

Our interest in this paper is the effect of lava dams on landscape evolution. We therefore base our study on an actual upland catchment that is known to be affected by multiple lava dams at its outlet, the Geren catchment in western Turkey (Van Gorp *et al.*, 2013). Our aim in this study is to elucidate the effect of damming events and uplift on the landscape evolution of a small upland catchment such as the Geren Catchment.

Specific objectives are:

1. to calibrate model parameters using reconstructed average net erosion over 300 ka; and
2. to compare the effect of different scenarios of driving factors on landscape evolution.

Study Site

The Geren catchment drains into the upper Gediz River, Western Turkey (Figure 1). Both rivers have mainly incised into Miocene fining-upward basinfills, containing gravels at the base, sands and silts of the Ahmetler formation in the middle part and lacustrine limestone deposits of the Ulubey formation on top (Seyitoglu, 1997). Fault-driven Plio-Pleistocene drainage diversion created the current Gediz River which incised into the readily erodible Ahmetler in the early Pleistocene (Maddy *et al.*, 2007). Since then, the upper Gediz River is responding to uplift with a time-averaged incision rate of 0·14 mm/a, while differential tectonics are not known to have occurred (Maddy *et al.*, 2012a). Initiation of volcanism in the early Pleistocene led to damming of the upper Gediz River system by lava flows in the early and middle Pleistocene and the Holocene at subsequently lower levels due to ongoing fluvial incision by the Gediz River (Richardson-Bunbury, 1996; Westaway *et al.*, 2004; Maddy *et al.*, 2012; Van Gorp *et al.*, 2013). The incision of the Gediz River in combination with repeated lava flows which filled and flowed down the Gediz valley until just downstream of the Gediz–Geren confluence control the base level of the Geren catchment. The top elevation of the middle Pleistocene lava flow remnants is around 40 m above current river level
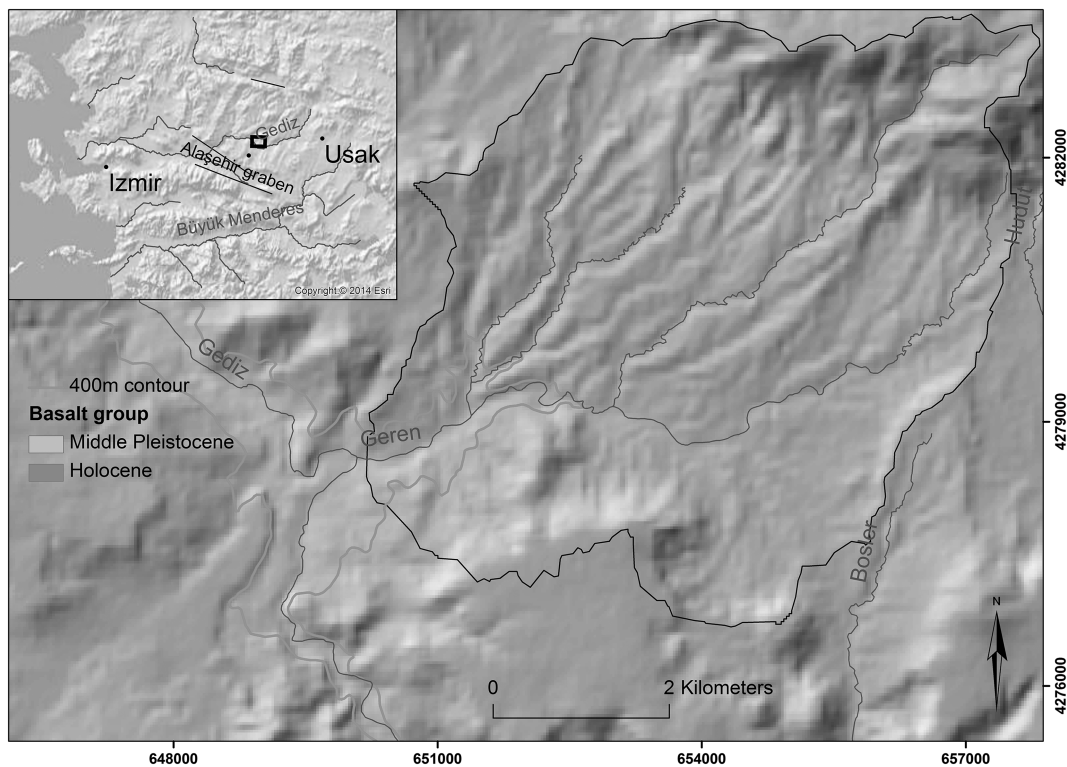

Figure 1. The Geren catchment and its confluence with the Gediz river, where several lavaflows filled and dammed the Gediz and Geren rivers (Van Gorp *et al.*, 2013). Inset shows its location in western Turkey at the shoulder of the Alaşehir graben. Coordinates are given in UTM-35 N, datum WGS-84. This figure is available in colour online at wileyonlinelibrary.com/journal/espl

and some are capped by fluvial deposits, indicating that the upstream Gediz reach and the Geren catchment have been dammed. While generally dam duration of the middle Pleistocene dams is unknown, their elevation is around 15–20 m. Dam duration of the youngest recognized dam is in the order of magnitude of 1 ka, where dam elevation in this case is approximately 20 m above current river level (Van Gorp *et al.*, 2013).

The Ulubey limestones now border the northern part of the Geren catchment in the form of a limestone scarpment (Figure 3). The larger part of the southern border of the Geren catchment consists of an early Pleistocene Lava plateau, capping unconsolidated Miocene Ahmetler sands, silts and gravels. The Geren catchment is dominantly incising into these Miocene basinfills, although at present, it hits underlying basement rocks near its outlet. In these reaches it mostly has a ridge-gully landscape, where ridges are often, but not always, capped by fluvial deposits derived from the upstream northern limestone plateau. These deposits either consist of coarse fluvial gravels, or of fine layered to laminated semi-horizontal sands and silts which can reach thicknesses of up to 20 m, indicating regime changes from more high energy fluvial conditions to low-energy conditions. Confined in the gullies, fluvial fill sequences are found at various levels. These aggradation–incision cycles are formed by at least 300 ka of catchment response to base level lowering of the Gediz River and we expect that repeated damming events have co-shaped the landscape evolution of the Geren catchment.

Methods

DEM extraction

Because the accuracy of the freely available SRTM and ASTER-GDEM was limited for the area, it was chosen to construct a digital elevation model (DEM) from stereo-satellite imagery. An ALOS-PRISM panchromatic imagery triplet with a pixel resolution of 2·5–3 m was obtained (Takaku and Tadono, 2009). The cloud-free forward, backward and nadir images, date from April 2007 and have an image scene centre latitude–longitude of 38·696 N and 28·714 E. Ground control points were measured using a Sokkia dGPS and 15 of them were used for dem extraction with the DEM extraction tool in ENVI 4·7. A systematic shift in the resulting DEM was corrected and spatial resolution was upscaled to 30 m for the purpose of the simulation in this paper.

PalaeoDEM creation

As an initial landscape for modelling, a palaeoDEM was created based on the 30 m ALOS-PRISM-derived current topography of the Geren catchment. Gradient and elevation of gently sloping ridge surface levels and crests suggest their correlation with a catchment outlet around 40 m above current outlet level. A simple reproducible method was used to extract the DEM. Current channel elevations were derived from the channel network of the DEM (Figure 2). Subsequently, All DEM gridcells which were more than 40 m above the elevation of the nearest channel were extracted (Figure 3). A palaeosurface base level was imposed 40 m above current outlet level, leading to a palaeo-outlet of 390 m. Surfaces were then interpolated between palaeosurface cells using Topo to Raster in ArcGIS, leading to a simplified 30 m resolution PalaeoDEM. Finally, sinks were filled using Planchon and Darboux (2002) sink fill method in SAGA-GIS, with a tangent of 0·01 degrees.

The gridcell elevations of the actual DEM were subtracted from the gridcell elevations of the constructed palaeoDEM. This led to

a total volume of $784 \times 10^6 \, \text{m}^3$ that was assumed removed in 300 ka. Using average bulk density of $1500 \, \text{kg m}^{-3}$, this corresponds to an approximate net erosion of $0\cdot97 \, \text{t ha}^{-1} \, \text{a}^{-1}$. This rate is low but within the lower range of erosion rates reported of some other uplifting areas (Safran *et al.*, 2005). The calculated erosion rate was used to calibrate model parameters as discussed below and in Figure 4.

Model framework

Reduced complexity LEM LAPSUS was used for simulations (Schoorl *et al.*, 2000, 2002; Temme *et al.*, 2009). LAPSUS is a cellular automaton that models a suite of geomorphic processes including water erosion and deposition and that can dynamically deal with non-spurious depressions (Temme *et al.*, 2006) and lakes (Van Gorp *et al.*, 2014). This makes it a suitable model for this study.

In LAPSUS, the multiple flow algorithm (Freeman, 1991; Quinn *et al.*, 1991) is used to route water down from a cell to each of its downstream neighbours. Water arriving in depressions is routed to the outlet of those depressions. Sediment transport capacity C (m) between two cells over distance s and timestep t (yr) is then calculated from the fractional discharge Q (m) and tangent of slope Λ (-) (Kirkby, 1971):

$$C_{s,t} = Q_{s,t}{}^m \cdot \Lambda_{s,t}^n \tag{1}$$

where parameters m and n are the discharge and slope exponent, respectively (Kirkby, 1987). The values of m and n reflect the type of runoff that is modelled. The sediment transport is then calculated based on the work of Foster and Meyer (1972, 1975).

$$S_{s,t} = C_{s,t} + \left(S_{0s,t} - C_{s,t}\right) \cdot e - ^{cellsize/h} \tag{2}$$

Where sediment in transport S (m) is a function of cell size (m), transport capacity C and erosion or sedimentation component h (m), compared with the amount of sediment already in transport S_0. If there is more sediment in transport than the transport capacity, deposition will occur and sedimentation component h is calculated as follows:

$$h_{s,t} = \frac{C_{s,t}}{P_{s,t} \cdot Q_{s,t} \cdot \Lambda_{s,t}} \tag{3}$$

where P (m^{-1}) is a sedimentation factor. High P-values indicate more potential to deposit sediment from transport, a low P indicates more potential to keep sediment in transport. However, P only becomes important when transport capacity on a cell is exceeded. If sediment already in transport is smaller than transport capacity, erosion will occur and h is calculated as follows:

$$h_{s,t} = \frac{C_{s,t}}{K_{s,t} \cdot Q_{s,t} \cdot \Lambda_{s,t}} \tag{4}$$

where K (m^{-1}) is an erodibility factor. Both K and P are lumped factors, representing surface characteristics for each cell of the catchment and are thus not empirically determined.

Parameter settings

In this study, erodibility factor K and sedimentation factor P are varied spatially according to geological substrate (Schoorl *et al.*, 2002). Initial K and P values were assigned to those areas underlain by Miocene alternating sands, silts and gravels. For the limestone plateau at the northern border, and the high basalt plateau at the southern border, K and P values were
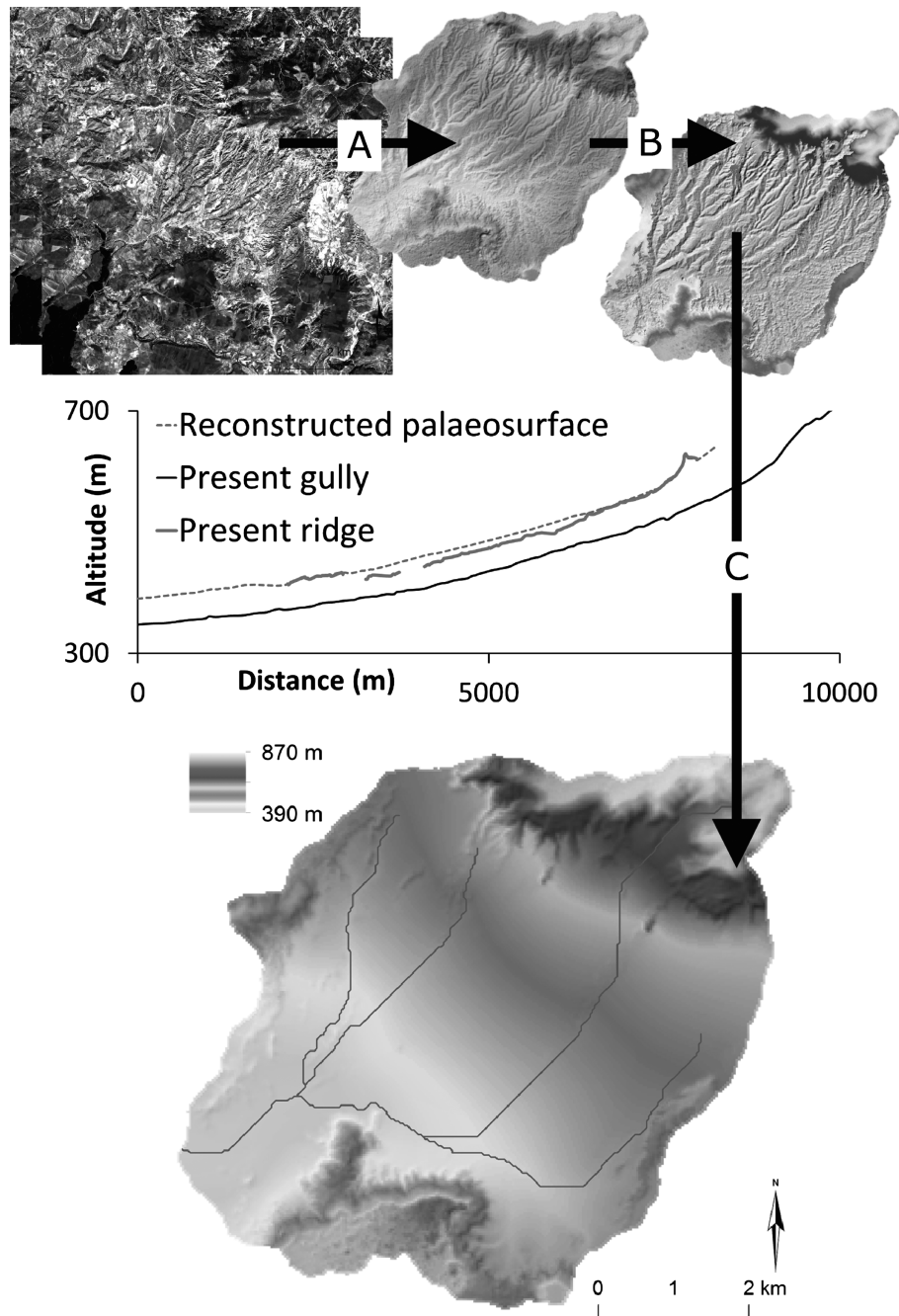
Figure 2. (A) DEM extraction from a forward and backward image pair of ALOS-PRISM panchromatic satellite imagery. (B) Extraction of those locations 40 m above current river level. (C) Interpolation of a paleoDEM area, using a 390 m elevation outlet area. This figure is available in colour online at wileyonlinelibrary.com/journal/espl

multiplied by 0·5 to mimic the more resistant bedrock (Table I, Figure 3). These resistant plateaus are both underlain by the Miocene sands, silts and gravel. The base of the northern plateau is estimated to be at 700 m, while the base height of the southern plateau is estimated to be at 580 m. Of course actual base heights are more variable, but a constant elevation is chosen for simplification reasons. This base height made it possible to change to the initial K and P values as soon as the bedrock was incised to its base height. In addition, cells with a redistributed sediment layer of at least 0·1 m thick were given a ten times higher K and P than the modelling substrate to mimic transport limited conditions of coarse bedload sediment. Furthermore, sedimentation factor P is four magnitudes higher than erodibility factor K (Table I). The reason for this large difference between P and K is that, on the long simulation timescale in this study, P is found to influence profile gradient of trunk streams, where higher P values generated more realistic profile

gradients. Parameters m and n were set at 1·65, which is in between typical values for hillslope processes and fluvial processes (Baartman et al., 2012b), while the runoff convergence factor $Pconv$, which controls if water follows a steepest descent path or a multiple flow path (Quinn et al., 1991), was set to 2 (Baartman et al., 2012a, our Table I).

Model calibration

Erodibility factor K was varied in a calibration exercise which had as its objective to minimize the difference between simulated net erosion and calculated net erosion. This was done by comparing net erosion from runs where uplift and three damming events were imposed, with net erosion calculated from the difference between the palaeoDEM and the current DEM. The value of K was varied from $1\cdot3 \times 10^{-5} \, \text{m}^{-1}$ to

Copyright © 2014 John Wiley & Sons, Ltd.

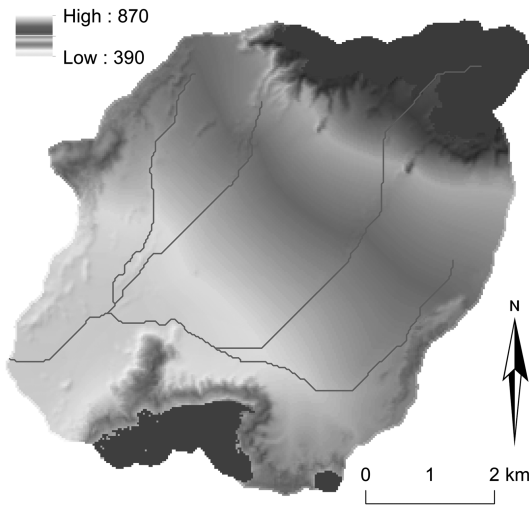Earth Surf. Process. Landforms, Vol. **40**, 888–900 (2015)

Figure 3. Simulation boundary conditions on top of the hillshaded palaeoDEM. The black rectangle shows the area where base level change occurs (both gradual and damming). Regions where K and P are multiplied by 0·5 are coloured. In the blue region (a plateau consisting of Miocene/Pliocene limestones), this multiplying occurs if cell elevation is higher than 700 m. In the red coloured region (a basalt plateau of early-Pleistocene age), this multiplying occurs if cell elevation is higher than 580 m. This figure is available in colour online at wileyonlinelibrary.com/journal/espl

$1·8 \times 10^{-5}\,\mathrm{m}^{-1}$, with steps of $1 \times 10^{-6}\,\mathrm{m}^{-1}$. Synchronously, P was varied from 0·13 to 0·18 with steps of 0·01 (Table I). The best fit K (and hence, P) values derived from the stepped calibration were selected for further analysis of spatial-temporal impacts. The base level lowering rate of $0·14\,\mathrm{mm}\,\mathrm{a}^{-1}$ was imposed on the outlet cells in the calibration phase.

Model scenarios

The model with the calibrated parameter set was run for different scenarios (Figure 4): (1) no change in external drivers; (2) three damming events at 50 ka, 150 ka and 250 ka; (3) a

Table I. LAPSUS model and parameter settings

Model settings

Model duration	300	[ka]
Effective rainfall	50	[mm a^{-1}]
Uplift rate	0·00014	[m a^{-1}]
Damming events	50, 150, 250	[ka]
Dam duration	1	[ka]
Dam elevation	20	[m]

LAPSUS parameter	Value		Step
m	1·65		
n	1·65		
$Pconv$	2		
K	$1·3 \times 10^{-5} - 1·8 \times 10^{-5}$	[m^{-1}]	1×10^{-6}
P	0·13–0·18	[m^{-1}]	0·01
$KP\_plateau$	$K \times 0·5$, $P \times 0·5$	[m^{-1}]	
KP_newsed	$K \times 10$, $P \times 10$	[m^{-1}]	
Grid size	30×30	[m]	
Timestep	1	[yr]	

constant base level lowering of the outlet cells by $0·14\,\mathrm{mm}\,\mathrm{a}^{-1}$, mimicking uplift-driven incision of the trunk river; and (4) scenario 2 and 3 combined, thus constant base level lowering with three damming events. The constant base level lowering and the lava dams were imposed at the catchment outlet. Base level lowering was imposed by lowering the outlet cells by $0·14\,\mathrm{mm}\,\mathrm{a}^{-1}$. Lava damming was imposed by adding 20 m to the westernmost part of the Geren outlet area (Figure 3) and dam duration was 1 ka, both based on field observations of the most recent damming event (Van Gorp *et al.*, 2013). Each damming event was ended by lowering the westernmost part of the outlet area by 20 m, 1 ka after the start of damming.

Output evaluation

To assess differences in spatial and temporal response between scenarios, four catchment properties were compared; (i) the
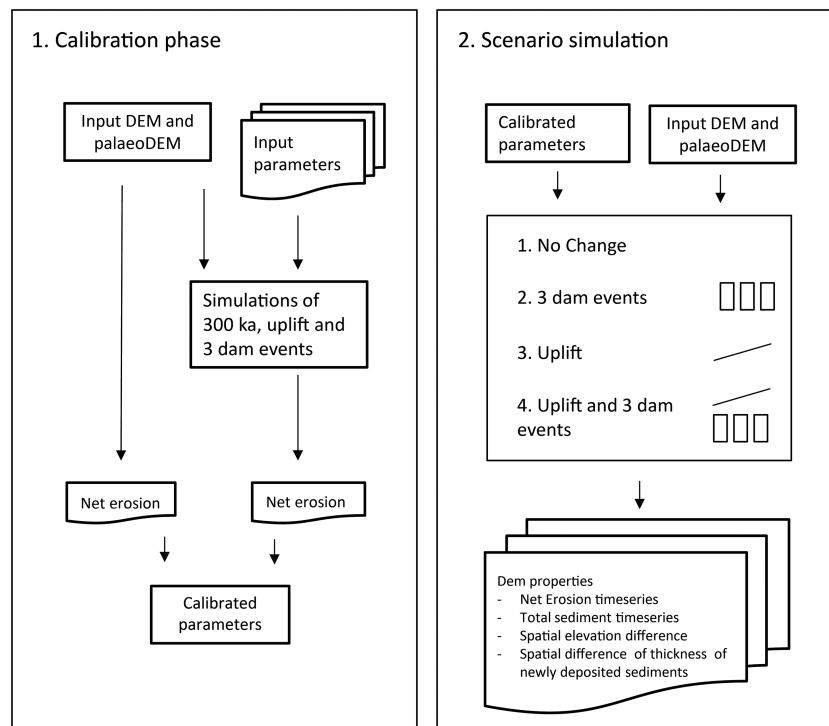

Figure 4. Experimental setup of model simulations.

time series of net erosion; (ii) profile evolution of the main gully; (iii) the difference in net erosion between scenarios; and (iv) the difference in storage of newly deposited sediments between scenarios. The latter two are shown separately because net erosion and sediment thickness on a cell can differ (Figure 5), resulting in different spatial patterns. Thus a cell can experience net erosion, but still contain a certain sediment thickness. The use of sediment thickness has the advantage that it gives information about sediment redistribution within the catchment.

Results

Step 1: Calibration

Average net erosion values for the calibration runs (Table II) show a gradual increase of net erosion with increasing K and P. The optimal parameter set has a net erosion of about $0.986 \, t \, ha^{-1} \, a^{-1}$, which is closest to the erosion rate from the palaeoDEM reconstruction. This optimal set is used for further scenario modelling.

Step 2: scenario modelling

For all four scenarios, a complex 1000 year averaged net erosion time series is simulated, in which erosion is not a linear or other simple function of driving factors (see Figure 6). Net erosion of the scenario 1 'No change' shows variable but generally declining annual net erosion. Further analysis of differences and similarities between different scenarios shows that: (i) average net erosion and its standard deviation are consistently higher for the scenarios with uplift than for scenarios without uplift; (ii) damming significantly changes annual net erosion and standard deviation of annual net erosion both with and without uplift; and (iii) temporal variability of scenarios 3 (uplift) and 4 (uplift with dams) differ significantly. In contrast, temporal variability is not significantly different between scenario 1 and scenario 2. The presence of uplift apparently

enhances the variability of net erosion. The net erosion signal often shows alternating periods of higher and lower variability, which indicates phases of enhanced activity.

Time series of sediment storage also show a difference in sediment dynamics between scenarios (Figure 7). Scenarios 1 and 2, without uplift, show a progressive although not a gradual increase in sediment storage, whereas scenario 3 and 4, with uplift, do not. In scenario 3, uplift only, quasi-periodic periods of sharp decrease in sediment storage occur which coincide with the high variability periods of net erosion. Damming has a positive effect on sediment storage both with and without uplift. Periods of sharp increase in sediment storage during damming events of scenario 2 at 50 ka, 150 ka, and 250 ka are directly related to lake formation and siltation behind the dam body. Scenario 4 shows a similar sharp increase of sediment storage after the dam at 50 ka, but at 150 ka and 250 ka this increase is absent. Differences between scenarios at other points in time are related to complex response caused by the initial differences in elevation and sediment distribution right after damming. To relate model results to the existing field setting, profile and spatial analysis of simulations will be carried out on scenarios 3 and 4, which include uplift.

River profile evolution generally shows a profile that is adapting to the constant uplift rate (Figure 8). A detachment limited profile is visible in the upper part of the catchment, where the low erodible plateau is incised. Below around

Table II. Total net erosion of scenario 4 (uplift and three damming events) for different calibration settings of K and P

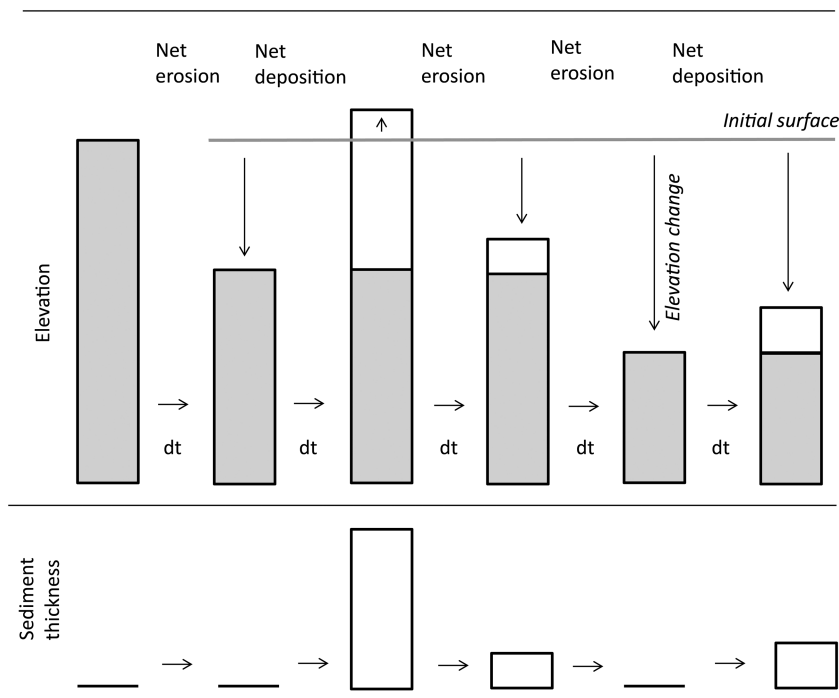| Parameter Erodibility K	Sediment factor P	Net erosion ($t \, ha^{-1} \, yr^{-1}$)
0.000013	0.13	0.851
0.000014	0.14	0.907
0.000015	0.15	0.921
0.000016	0.16	0.986
0.000017	0.17	1.023
0.000018	0.18	1.036

Figure 5. Schematic diagram of elevation change versus thickness of newly deposited sediments of a cell over time.
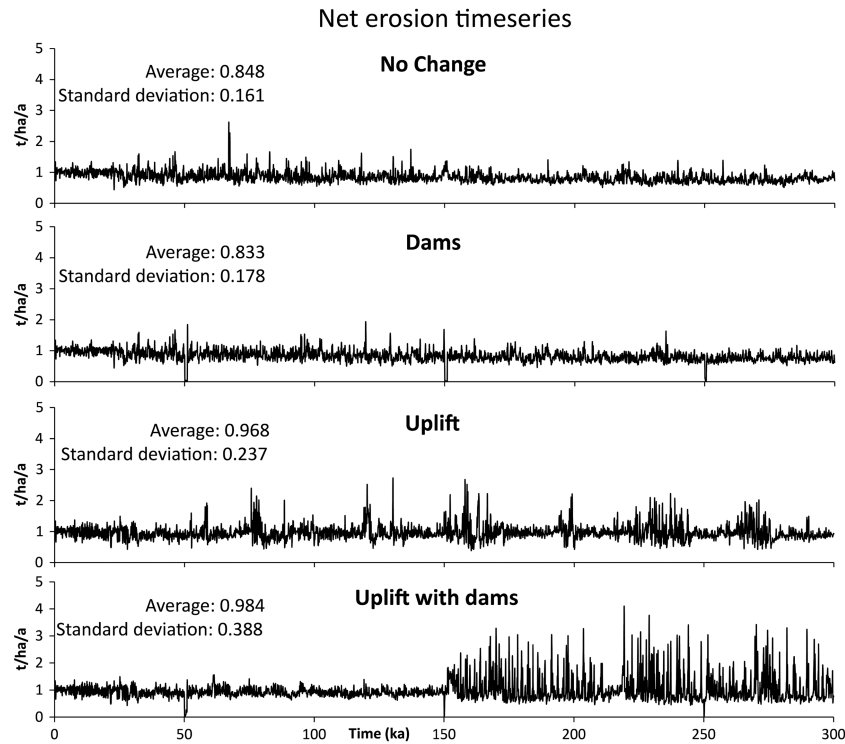
Net erosion timeseries

Figure 6. Time series of 1000 year averaged net erosion for scenarios 1–4 for the optimal parameter set.
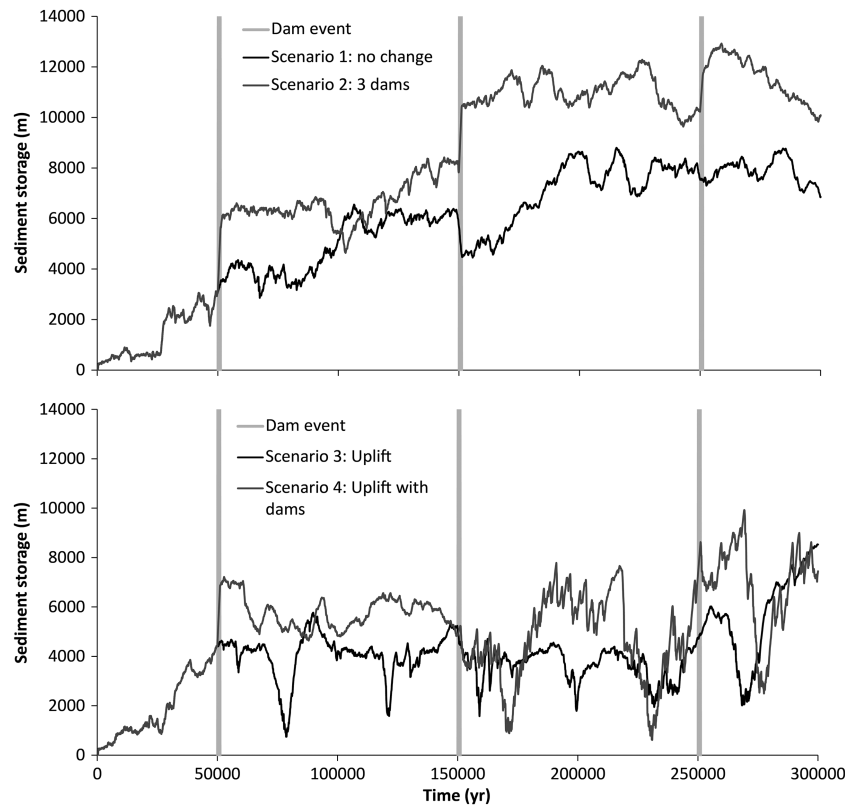

Figure 7. Time series of sediment storage. Top: Scenario 1 and 2, Bottom: scenario 3 and 4.

500 m altitude, sediment loads become higher and the profile forms a more linear to convex shape. Different knickpoints are visible which migrate upstream, or profile sections aggrade in the downstream direction. For instance, top-down driven aggradation is visible when comparing the profiles of 51 ka and 100 ka at an elevation around 500 m. Comparison of profile evolution between scenarios 3 and 4 reveals differences

in elevation of up to 15 m within the trunk gully. Infilling right after damming is visible at 51, 151 and 251 ka.

Spatial patterns through time are assessed by looking at differences between elevation maps of scenarios (thus, differences in net erosion) and differences between sediment storage maps of scenarios. Difference between elevation maps are shown in Figures 9 and 10. At *t* = 51001, one year after removal of the
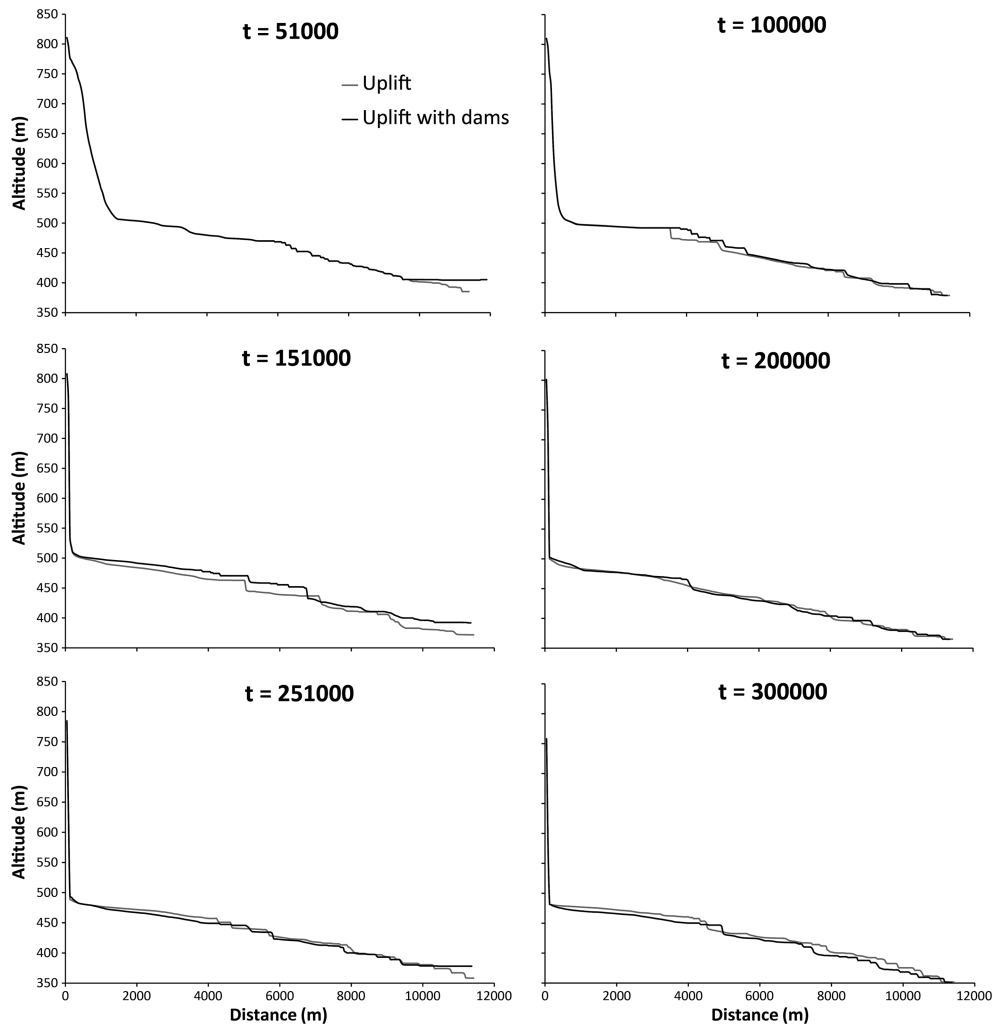
Figure 8. Longitudinal profiles of uplift and uplift with dams of the principal trunk gully at several timesteps. Dammings occur at $t = 50$ to 51 ka, 150 to 151 ka and 250 to 251 ka.

first dam, the sediment storage behind the dam is clearly visible as a positive difference. This difference extends to upstream regions via the main gully systems when looking at $t = 75000$ and onwards until $t = 151001$. This visual difference is mostly positive, thus, net erosion is less for scenario 4 'uplift with three damming events' than for scenario 3 'uplift'. However, negative differences occur in different gully systems at different points in time. For instance, negative differences occur near the catchment outlet. This is due to stream rerouting on top of the lake sediments and post-dam incision in scenario 4. Over time, this incision shortcuts local streams, creating more incision and thus a negative elevation difference. At the time of removal of the third dam at $t = 251001$ and onwards, positive differences extend to slopes adjacent to gullies while the gullies themselves switch to a negative difference.

Snapshots through time of sediment storage difference maps between scenario 4 and 3 again show the direct effect of damming due to lake sediment storage behind the first dam, right after its removal at $t = 51001$ (Figure 11). Storage difference rapidly extends to upstream gullies and sometimes switches from a positive to a negative difference. The difference due to the sediment body directly behind the dam gradually diminishes over time. After the second and third dam event at $t = 151001$ and $t = 251001$, the difference due to sediment storage being confined to the trunk gully. The changes from positive to negative differences through space and time indicate sediment waves which are active at different moments for the different scenarios.

In summary, results show a clear difference in net erosion and sediment storage between uplift and no uplift scenarios, while the difference between dam and no dam scenarios is especially expressed when looking at time series and spatial patterns of net erosion and sediment storage. More sediment is stored when damming occurs. This is due to remnants of storage directly behind the dam body, and to upstream storage in the trunk and other gullies.

Discussion

The simulated time series of net erosion and sediment storage all show autogenic behaviour and nonlinearity (cf. Coulthard and Van De Wiel, 2007). The occurrence of this complex LAPSUS output has been discussed in recent other papers and is partly ascribed to landscape complexity and autogenic feedbacks (Van Gorp *et al.*, 2014; Schoorl *et al.*, 2014). However the type of behaviour differs between scenarios. The difference in pattern between the variability in time series of net erosion between scenario 1 and 3 (no uplift and uplift) suggests that uplift shifts complex response into another state. Gradual base level lowering causes high variability and low variability net erosion phases to alternate quasi-periodically, which suggests that autogenic behaviour can generate non-climatically driven cyclic patterns in sediment archives. Rather, these patterns are driven by the episodic build-up and release of sediments by
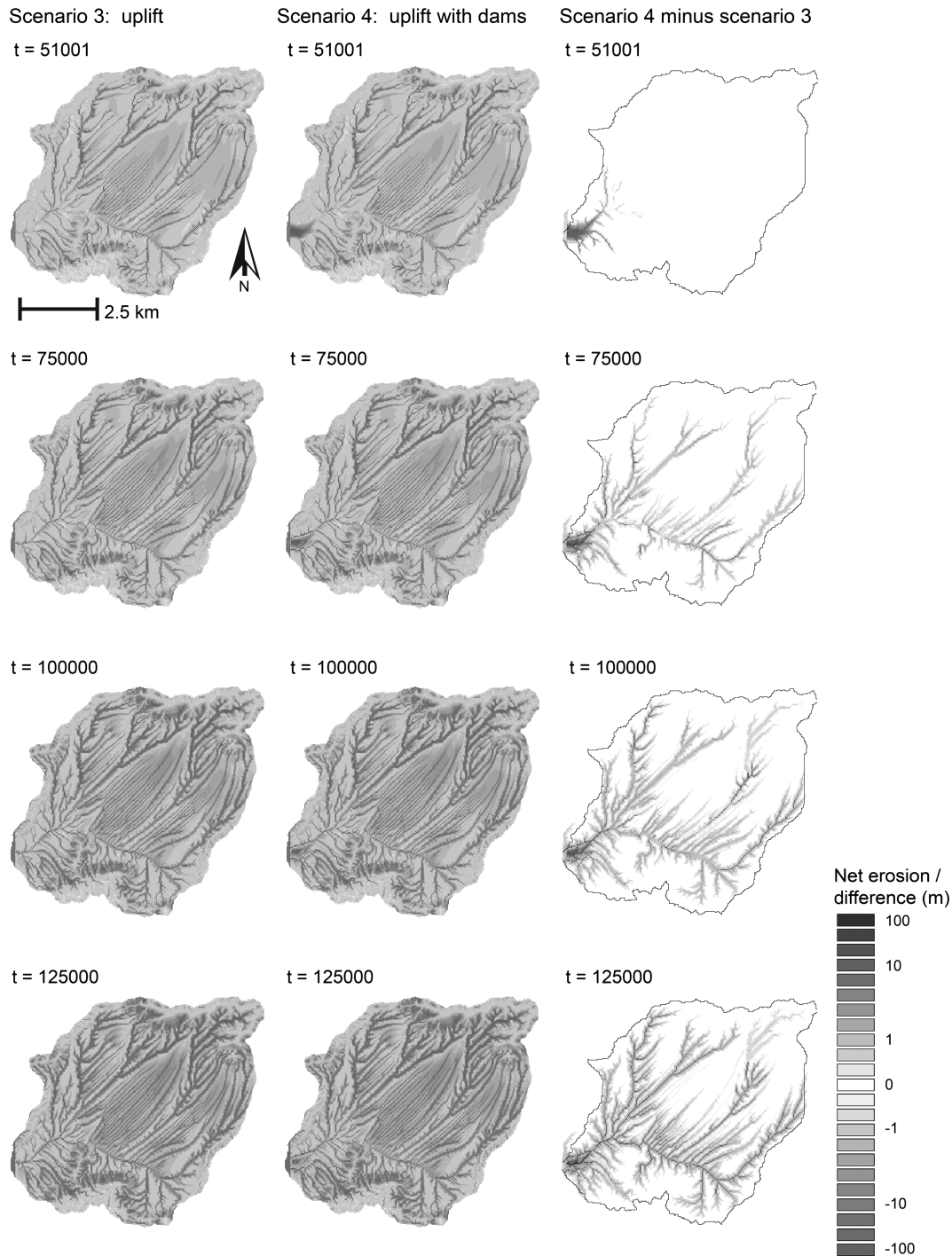
Figure 9. Maps of elevation change since the start of the run (Column A and B) and difference in elevation change between scenario 4 'Uplift with three damming events' and scenario 3 'uplift' (Column C) for *t* = 51 001, right after the first dam between 50 000 and 51 000 yr, to *t* = 125 000. This figure is available in colour online at wileyonlinelibrary.com/journal/espl

the catchment, which is controlled by catchment topography, but apparently unlocked by gradual base level lowering.

Most of the time, response to damming is not visible in the net erosion signal, suggesting shredding of the dam signal owing to sediment redistribution (a mechanism suggested by Jerolmack and Paola, 2010). However, after the second damming in scenario 4, the net erosion signal shifts from a weakly variable to a highly variable signal. This is visible in the sediment storage signal as an increase in variation. Increased sedimentation during damming is the most direct effect of lava dams on spatial catchment evolution (Figures 9–11), as further documented by numerous reconstruction studies (Ely *et al.*, 2012; Van Gorp *et al.*, 2013).

The more interesting effect in the simulations is upstream migration of elevation differences between dam and non-dam

scenarios (Figures 9 and 10). This migration starts at the start of the first damming at 50 ka and extends over an ever increasing area of the catchment until the end of the 300 ka simulation. Differences first arise in the main gullies after which they extend to smaller gullies and slopes along gullies. The generally lower net erosion in the dam scenario extends to upstream regions until *t* = 150 000. However, from *t* = 200 000 and onwards (Figure 9), a negative difference extends into all main gullies. This results in channel–hillslope decoupling with a positive difference in smaller gullies and slopes and a negative difference in the main gullies. This indicates an increase in local relief in scenario 4 'uplift with dams' compared with scenario 3 'uplift'. This suggests that the damming effect amplifies the decoupling between main gullies and their tributaries and
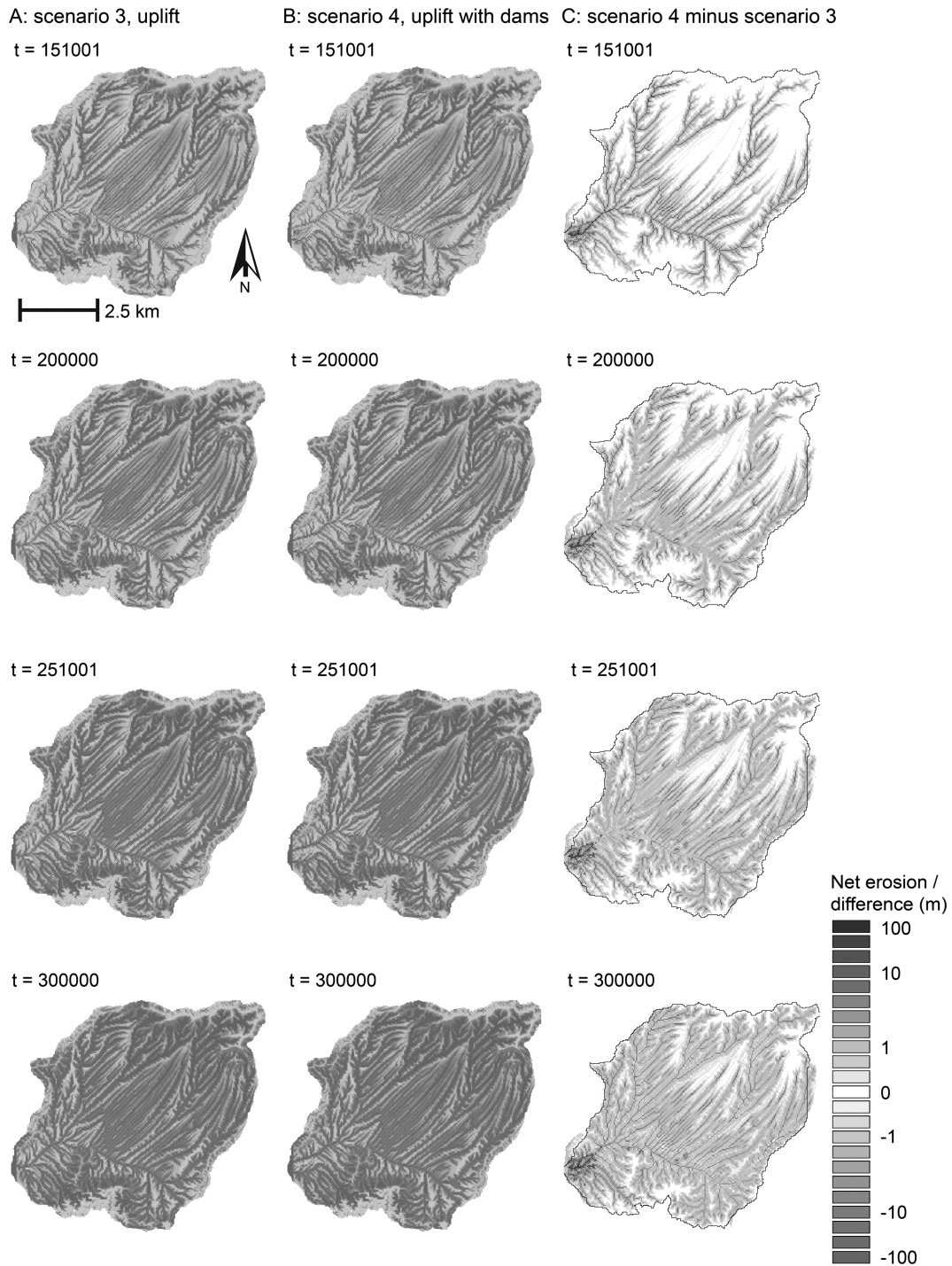
Figure 10. Maps of elevation change since the start of the run (Column A and B) and difference in elevation change between scenario 4 'Uplift with three damming events' and scenario 3 'uplift' (Column C) for $t = 151\,001$ to $t = 300\,000$. Damming events occur at 50 000 to 51 000 yr, 150 000 to 151 000 yr and 250 000 to 251 000 yr. This figure is available in colour online at wileyonlinelibrary.com/journal/espl

slopes. Furthermore, it demonstrates a legacy effect in the landscape over timescales of 300 ka. The more complex signal of spatial sediment storage difference (Figure 11) is owing to the fact that the location of gully stretches containing sediments differs through time, which can lead to zero difference between scenario 3 and 4 at one timestep, while a large difference was present at an earlier timestep. Nevertheless, differences of sediment storage migrate upstream at least until $t = 125\,000$ ka. Drainage rearrangement after the first damming (50 ka) affects local stream paths and stream lengths and over time affects the stream length of the trunk gullies as well. The main gully is rerouted to the north of the dam body, shortening the trunk stream length. This difference in drainage path of local and trunk streams can play a role in increasing long-term incision

in scenario 4 'uplift with three damming events', 150 ka after occurrence of rearrangement, around 200 ka. The damming therefore does not only cause a delay and decoupling of different river reaches, it can also lead to an amplified incision rate.

Model sensitivity

The sensitivity of simulation outputs to small changes in parameters was assessed by an analysis of the outputs for the parameter sets that were not selected after calibration. The average and variation of net erosion for the parameter settings that were not selected after calibration show similar trends to those of the optimal parameter set depicted in Figure 6. However, the exact shape of
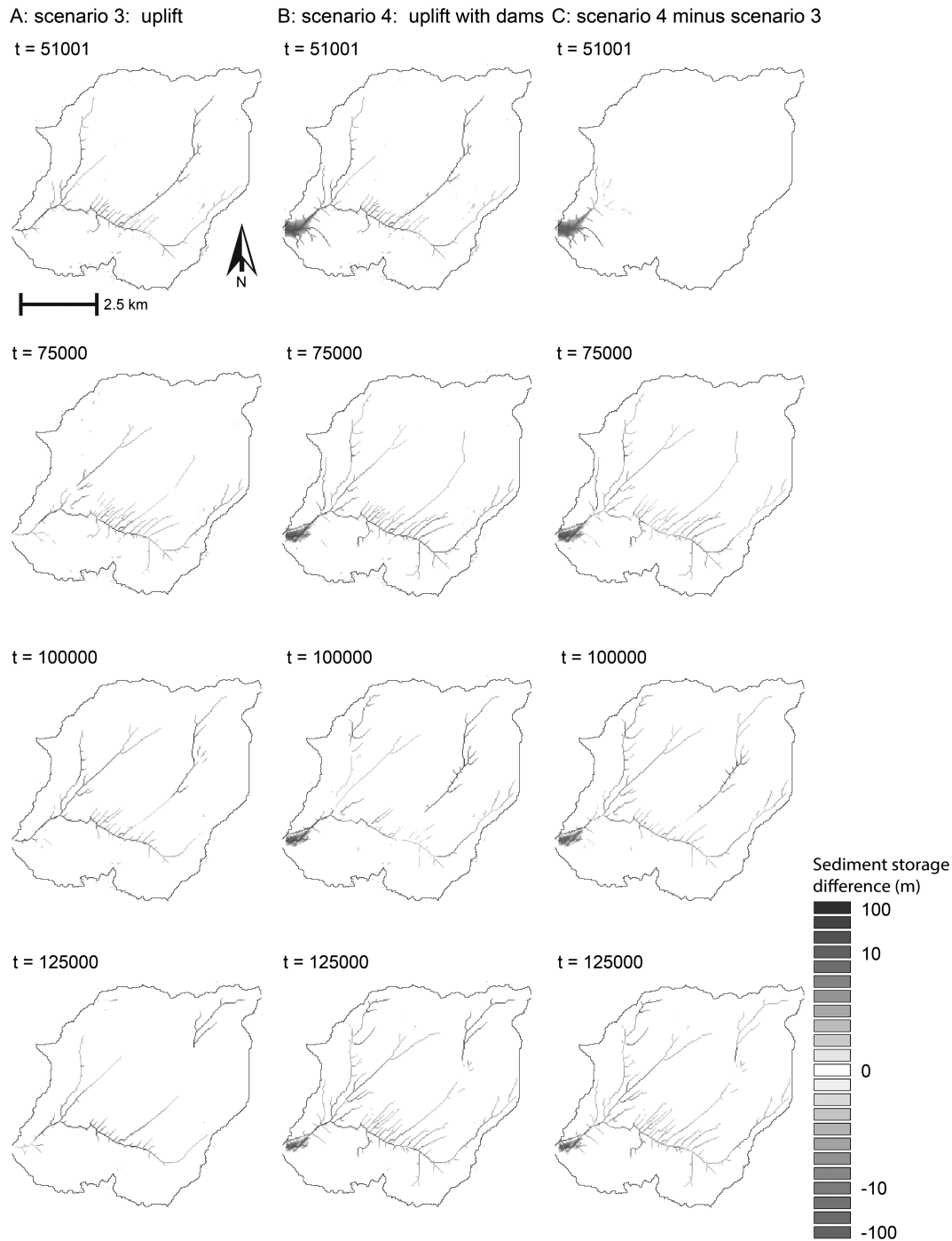
Copyright © 2014 John Wiley & Sons, Ltd.

Earth Surf. Process. Landforms, Vol. **40**, 888–900 (2015)

A: scenario 3: uplift   B: scenario 4: uplift with dams   C: scenario 4 minus scenario 3

Figure 11. Snapshots of sediment storage of scenario 3 'uplift' (column A) and scenario 4 'Uplift with three damming events' (column B) and their difference (column C) for *t* = 51001, 75 000, 100 000 and 151 001 ka. parameter setting *K* = 0·000016, *P* = 0·16. This figure is available in colour online at wileyonlinelibrary.com/journal/espl

the time series is sensitive to parameter settings in a complex way. Likewise, upstream migration of net erosion differences (Figures 9 and 10) occurs in all parameter settings, but the exact pattern is dependent on parameter settings. Thus, exact locations of positive and negative differences vary between parameter settings. Nevertheless, for all parameter sets, damming events in an uplift driven landscape have a similar long- term effect on landscape evolution as discussed above for the calibrated parameter set.

Erodibility parameter *K* and sedimentation parameter *P* have been used for calibration. Generally, *P* has much less influence on total erosion values than *K*. Sensitivity plots of *K* and *P* are described in Baartman *et al.* (2012a) and Schoorl *et al.* (2014) and indicate that sedimentability factor *P* influences resedimentation and floodplain dynamics, while hardly influencing total erosion (Schoorl *et al.*, 2014).

Model setup limitations

In our simulation, damming and dam removal are imposed and occur instantaneously. Damming is simplified by elevating the outlet cells by 20 m. After 1000 yr, these cells are instantaneously lowered by 20 m, thus mimicking sudden dam removal or breach. The reason for this simplified imposition of damming is that we simulate response of the Geren tributary catchment on dams in its trunk valley, the Gediz. The Gediz controls damming and dam removal and it is not aimed to model this process.

Within this experiment, the initial PalaeoDEM construction is based on simplified assumptions. The main assumption is the correspondence of current crest elevations and gradients to palaeotopography. The resulting smoothed surface is a

simplification of the actual palaeosurface and contains four main parallel subbasins, which, although containing a simplified straight morphology, roughly coincide with basin orientation of the current DEM (Figure 2). We chose to use this surface to keep model inputs as clean and simple as possible to demonstrate differences in complex response between the different scenarios. We do acknowledge that a better uncertainty analysis of initial surface conditions would be advisable.

Several external climate related controls which are known to have varied within the modelled temporal extent have been held constant in our simulations. Effective rainfall is held constant over the 300 ka simulation period, although over this temporal extent, climate change is thought to play a significant role (Tzedakis *et al.*, 2006 for the Eastern Mediterranean). The reasons to keep rainfall constant are first to keep the simulation results as generic as possible, and second, there are large uncertainties associated with rainfall reconstructions. Rainfall reconstructions on these timescales often rely on reconstructions of sea surface temperature curves and evaporation reconstructions rely on $\delta^{18}O$ curves. Successful rainfall reconstructions have been made for systems where a direct link with a certain oceanic system is established (e.g. the atlantic ocean, Stemerdink *et al.*, 2010; Viveen *et al.*, 2013). However, such a reconstruction is more problematic for more continental systems. Another external control which is not varied is vegetation cover, which influences the erodibility of the landscape. This was done as well to keep outputs as widely applicable as possible.

Although keeping these parameters constant implies a significant simplification compared with actual landscape evolution, it allows a clean assessment of the impact of changing base level scenarios on an upland catchment. This approach is widely taken in landscape evolution modelling literature (Coulthard and Van De Wiel, 2007; Tucker, 2009; Temme *et al.*, 2011).

One other step towards a clean assessment that is often taken in literature, is imposing equilibrium conditions on the study area before the start of comparative simulations (such as suggested by Tucker, 2009). This was not done in the present study because the imposition of equilibrium conditions, where erosion equals uplift averaged over the study area, would result in two different starting landscapes for the non-uplift and uplift scenarios. This would have meant that results could not be compared between these scenarios. Since such comparison was our objective, no equilibrium was imposed. In the uplift scenarios, the catchment is not in a steady state equilibrium. The average long-term catchment wide erosion rate does not change significantly over 300 ka (Figure 6). It is, however, lower than the outlet base level change. The outlet lowering rate is constant and 0·14 mm yr^{-1}, while the average erosion rate is around 0·06 mm yr^{-1} and does not show a significant trend. This difference is expressed in the increase of relief in the catchment, which is thus not in topographical steady-state (Goren *et al.*, 2014). It is however not our aim to reach a steady state in this study as we think that knowledge of response of non-steady state landscapes to external drivers is valuable due to their common occurrence (Tucker, 2009).

Conceptually, it is currently debated whether equilibrium conditions exist in actual field conditions (Phillips, 2014). Both field and modelling studies suggest that the establishment of equilibrium in a wide variety of geological and climatic settings takes millions of years of constant forcing (Goren *et al.*, 2014). Such constancy is rare. In the upper Gediz basin where this study is based, equilibrium conditions did not exist 300 ka ago nor do they in the actual landscape.

Conclusion

Landscape evolution modelling revealed that lava damming events of 1 ka duration can have demonstrable net effects on catchment evolution on a 100 ka scale. Furthermore, it demonstrated that adding gradual base lowering as a boundary condition unlocks a different, more variable autogenic catchment behaviour compared with absence of base level lowering. Model parameters were calibrated to net erosion rates over 300 ka that were derived from palaeoDEM reconstruction of the small (45 km^2) Geren catchment which is known to have endured several damming events. Results showed that upstream migration of net erosion difference between scenarios with and without damming events is still ongoing 250 ka after the first dam event. At first, trunk gullies show less net erosion in the scenario with damming events compared with the scenario without damming events. Then this effect migrates to smaller gullies and local slopes. Finally, an intrinsic incision pulse in the dam scenario results in a higher net erosion of trunk gullies while decoupled local slopes are still responding to the pre-incision landscape. Sediment storage differences occurred on a 100 ka scale as well. However, they behaved in a complex manner due to different timings of the migration of sediment waves through gullies for each scenario. Although the exact spatial and temporal sequence of erosion and deposition events is sensitive to parameters and the initial palaeoDEM is uncertain, this model study demonstrates how short-lived events such as a lava dam can have long lived effects on catchment evolution. These events can even amplify the erosion rates due to prolonged decoupling of channels and slopes.

References

Baartman JEM, Temme AJAM, Schoorl JM, Braakhekke MH, Veldkamp TA. 2012b. Did tillage erosion play a role in millennial scale landscape development? *Earth Surface Processes and Landforms* **37**: 1615–1626.

Baartman JEM, Van Gorp W, Temme AJAM, Schoorl JM. 2012a. Modelling sediment dynamics due to hillslope–river interactions: incorporating fluvial behaviour in landscape evolution model LAPSUS. *Earth Surface Processes and Landforms* **37**: 923–935.

Coulthard TJ, Lewin J, Macklin MG. 2005. Modelling differential catchment response to environmental change. *Geomorphology* **69**: 222–241.

Coulthard TJ, Lewin J, Macklin MG. 2007. Non-stationarity of basin scale sediment delivery in response to climate change. In Developments in Earth Surface Processes, Habersack H, Piegay H, Rinaldi M (eds). Elsevier: Amsterdam; 315–331.

Coulthard TJ, Van De Wiel MJ. 2007. Quantifying fluvial non linearity and finding self organized criticality? Insights from simulations of river basin evolution. *Geomorphology* **91**: 216–235.

Ely LL, Brossy CC, House PK, Safran EB, O'Connor JE, Fenton CR, Bondre NR, Orem CA, Grant GE, Henry CD, Turrin BD. 2012. Owyhee River intracanyon lava flows: does the river give a dam? *Bulletin of the Geological Society of America* **124**: 1667–1687.

Fenton CR, Webb RH, Cerling TE. 2006. Peak discharge of a Pleistocene lava-dam outburst flood in Grand Canyon, Arizona, USA. *Quaternary Research* **65**: 324–335. DOI: 10.1016/j.yqres.2005.09.006

Foster GR, Meyer LD. 1972. A closed-form soil erosion equation for upland areas. In Sedimentation: Symposium to Honour professor H.A Einstein, Shen HW (ed). Colorado State University, Fort Collins, CO, 190–207.

Foster GR, Meyer LD. 1975. Mathematical simulation of upland erosion by fundamental erosion mechanics. *Sediment-Yield Workshop, Present and Prospective Technol for Predict Sediment Yields and Sources, Proc, USDA Sediment Lab*: **190–207**.

Freeman TG. 1991. Calculating catchment area with divergent flow based on a regular grid. *Computers and Geosciences* **17**: 413–422.

Goren L, Willett SD, Herman F, Braun J. 2014. Coupled numerical-analytical approach to landscape evolution modeling. *Earth Surface Processes and Landforms* **39**: 522–545. DOI: 10.1002/esp.3514

Hancock GR, Coulthard TJ. 2012. Channel movement and erosion response to rainfall variability in southeast Australia. *Hydrological Processes* **26**: 663–673.

Jerolmack DJ, Paola C. 2010. Shredding of environmental signals by sediment transport. *Geophysical Research Letters* **37**. DOI: 10.1029/2010GL044638

Kirkby MJ. 1971. Hillslope process-response models based on the continuity equation. In Slopes, Forms and Processes. Transactions of the IBG. Special publication,Brunsden D (ed). Royal Geographical Society: London; 15–30.

Kirkby MJ. 1987. Modelling some influences of soil erosion, landslides and valley gradient on drainage density and hollow development. *Catena Supplement* **10**: 1–14.

Korup O, Densmore AL, Schlunegger F. 2010. The role of landslides in mountain range evolution. *Geomorphology* **120**: 77–90.

Korup O, Strom AL, Weidinger JT. 2006. Fluvial response to large rock-slope failures: examples from the Himalayas, the Tien Shan, and the Southern Alps in New Zealand. *Geomorphology* **78**: 3–21.

Maddy D, Demir T, Bridgland DR, Veldkamp A, Stemerdink C, van der Schriek T, Schreve D. 2007. The Pliocene initiation and early Pleistocene volcanic disruption of the palaeo-Gediz fluvial system, western Turkey. *Quaternary Science Reviews* **26**: 2864–2882.

Maddy D, Demir T, Veldkamp A, Bridgland DR, Stemerdink C, van der Schriek T, Schreve D. 2012a. The obliquity-controlled early Pleistocene terrace sequence of the Gediz river, western Turkey: a revised correlation and chronology. *Journal of the Geological Society* **169**: 67–82. DOI: 10.1144/0016-76492011-011

Maddy D, Veldkamp A, Jongmans AG, Candy I, Demir T, Schoorl JM, van der Schriek T, Stemerdink C, Scaife RG, van Gorp W. 2012. Volcanic disruption and drainage diversion of the palaeo-Hudut River, a tributary of the Early Pleistocene Gediz River, Western Turkey. *Geomorphology* **165–166**: 62–77.

Peeters I, Van Oost K, Govers G, Verstraeten G, Rommens T, Poesen J. 2008. The compatibility of erosion data at different temporal scales. *Earth and Planetary Science Letters* **265**: 138–152.

Phillips JD. 2006. Evolutionary geomorphology: tThresholds and non-linearity in landform response to environmental change. *Hydrology and Earth System Sciences* **10**: 731–742.

Phillips JD. 2014. Thresholds, mode switching, and emergent equilibrium in geomorphic systems. *Earth Surface Processes and Landforms* **39**: 71–79. DOI: 10.1002/esp.3492

Planchon O, Darboux F. 2002. A fast, simple and versatile algorithm to fill the depressions of digital elevation models. *Catena* **46**: 159–176.

Quinn P, Beven K, Chevallier P, Planchon O. 1991. The prediction of hillslope flow paths for distributed hydrological modelling using digital terrain models. *Hydrological Processes* **5**: 59–79.

Richardson-Bunbury JM. 1996. The Kula volcanic field, western Turkey: the development of a Holocene alkali basalt province and the adjacent normal-faulting graben. *Geological Magazine* **133**: 275–283.

Roach IC, Hill SM, Lewis AC. 2008. Evolution of a small intraplate basaltic lava field: Jerrabattgulla creek, upper shoalhaven river catchment, southeast New South Wales. *Australian Journal of Earth Sciences* **55**: 1049–1061. DOI: 10.1080/08120090802266543

Safran EB, Bierman PR, Aalto R, Dunne T, Whipple KX, Caffee M. 2005. Erosion rates driven by channel network incision in the Bolivian Andes. *Earth Surface Processes and Landforms* **30**: 1007–1024.

Sawaske SR, Freyberg DL. 2012. A comparison of past small dam removals in highly sediment-impacted systems in the US. *Geomorphology* **151–152**: 50–58.

Schoorl JM, Sonneveld MPW, Veldkamp A. 2000. Three-dimensional landscape process modelling: the effect of DEM resolution. *Earth Surface Processes and Landforms* **25**: 1025–1034.

Schoorl JM, Temme AJAM, Veldkamp T. 2014. Modelling centennial sediment waves in an eroding landscape - catchment complexity. *Earth Surface Processes and Landforms* **39**: 1526–1537.

Schoorl JM, Veldkamp A, Bouma J. 2002. Modeling water and soil redistribution in a dynamic landscape context. *Soil Science Society of America Journal* **66**: 1610–1619.

Schumm SA. 1979. Geomorphic thresholds: the concept and its applications. *Transactions. Institute of British Geographers* **4**: 485–515.

Seyitoglu G. 1997. Late Cenozoic tectono-sedimentary development of the Selendi and Uşak-Güre basins: a contribution to the discussion on the development of east-west and north trending basins in western Turkey. *Geological Magazine* **134**: 163–175.

Stemerdink C, Maddy D, Bridgland DR, Veldkamp A. 2010. The construction of a palaeodischarge time series for use in a study of fluvial system development of the Middle to Late Pleistocene Upper Thames. *Journal of Quaternary Science* **25**: 447–460.

Takaku J, Tadono T. 2009. High resolution DSM generation from ALOS PRISM - Status updates on over three year operations. In *International Geoscience and Remote Sensing Symposium (IGARSS)*, III769-III772, Cape Town, 2009.

Temme AJAM, Baartman JEM, Schoorl JM. 2009. Can uncertain landscape evolution models discriminate between landscape responses to stable and changing future climate? A millennial-scale test. *Global and Planetary Change* **69**: 48–58.

Temme AJAM, Claessens L, Veldkamp A, Schoorl JM. 2011. Evaluating choices in multi-process landscape evolution models. *Geomorphology* **125**: 271–281. DOI: 10.1016/j.geomorph.2010.10.007

Temme AJAM, Schoorl JM, Veldkamp A. 2006. Algorithm for dealing with depressions in dynamic landscape evolution models. *Computers and Geosciences* **32**: 452–461.

Temme AJAM, Veldkamp A. 2009. Multi-process late quaternary landscape evolution modelling reveals lags in climate response over small spatial scales. *Earth Surface Processes and Landforms* **34**: 573–589.

Tucker GE. 2009. Natural experiments in landscape evolution. *Earth Surface Processes and Landforms* **34**: 1450–1460.

Tucker GE, Hancock GR. 2010. Modelling landscape evolution. *Earth Surface Processes and Landforms* **35**: 28–50 DOI: 10.1002/esp.1952

Tucker GE, Lancaster ST, Gasparini NM, Bras RL, Rybarczyk SM. 2001. An object-oriented framework for distributed hydrologic and geomorphic modeling using triangulated irregular networks. *Computers and Geosciences* **27**: 959–973.

Tzedakis PC, Hooghiemstra H, Pälike H. 2006. The last 1·35 million years at Tenaghi Philippon: revised chronostratigraphy and long-term vegetation trends. *Quaternary Science Reviews* **25**: 3416–3430.

Van De Wiel MJ, Coulthard TJ, Macklin MG, Lewin J. 2011. Modelling the response of river systems to environmental change: progress, problems and prospects for palaeo-environmental reconstructions. *Earth-Science Reviews* **104**: 167–185.

Van Gorp W, Veldkamp A, Temme AJAM, Maddy D, Demir T, Van der Schriek T, Reimann T, Wallinga J, Wijbrans J, Schoorl JM. 2013. Fluvial response to Holocene volcanic damming and breaching in the Gediz and Geren rivers, western Turkey. *Geomorphology* **201**: 430–448. DOI: 10.1016/j.geomorph.2013.07.016

Van Gorp W, Temme AJAM, Baartman JEM, Schoorl JM. 2014. Landscape evolution modelling of naturally dammed rivers. *Earth Surface Processes and Landforms* **39**: 1587–1600.

Veldkamp A, Schoorl JM, Wijbrans JR, Claessens L. 2012. Mount Kenya volcanic activity and the Late Cenozoic landscape reorganisation in the upper Tana fluvial system. *Geomorphology* **145–146**: 19–31.

Viveen W, Schoorl JM, Veldkamp A, van Balen RT, Desprat S, Vidal-Romani JR. 2013. Reconstructing the interacting effects of base level, climate, and tectonic uplift in the lower Miño River terrace record: a gradient modelling evaluation. *Geomorphology* **186**: 96–118.

Wainwright J. 2006. Degrees of separation: hillslope-channel coupling and the limits of palaeohydrological reconstruction. *Catena* **66**: 93–106. DOI: 10.1016/j.catena.2005.07.016

Westaway R, Pringle M, Yurtmen S, Demir T, Bridgland D, Rowbotham G, Maddy D. 2004. Pliocene and Quaternary regional uplift in western Turkey: the Gediz River terrace staircase and the volcanism at Kula. *Tectonophysics* **391**: 121–169.

Copyright © 2014 John Wiley & Sons, Ltd.

Earth Surf. Process. Landforms, Vol. **40**, 888–900 (2015)